Engineering Technology Open Access Journal

Juniper Publishers key to the Researchers

Research Article
Volume 6 Issue 4 - August 2025
DOI: 10.19080/ETOAJ.2025.06.555693

Eng Technol Open Acc

Chemical Analysis of a Tritium Plasma Graphene Interactions with Stochastic Approaches

Alper Pahsa*

HAVELSAN Inc, Ankara, Turkey

Submission: August 14, 2025; **Published:** August 22, 2025

***Corresponding author:** Alper Pahsa, HAVELSAN Inc, Ankara, Turkey

Abstract

The chemical processes of the tritium plasma graphene wall contacts must be investigated when building a Tokamak fusion reactor. The enormous heat and energy of fusion reactions can alter how the reactors' physical surfaces form. If graphene is chosen for the fusion reactor's construction, this happens when the atoms of the fusion tritium fuel enter the wall structures. Tritium plasma ions penetrate the graphene crystal's surface in this experiment. Tritium plasma ions with energies ranging from 5 to 35 keV can penetrate graphene crystal surfaces with the aid of molecular dynamics, and the chemical reactions that result are examined using stochastic methods based on Shannon entropy parameters based on kinetic energy.

Keywords: Chemical process of PMI; Tritium Plasma Graphene Interaction; Molecular Dynamics of PMI

Introduction

Because of its almost infinite fuel supply and low radiation levels, fusion reactors are perfect for space technologies and energy production. These reactors generate helium, neutrons, and other particles through hydrogen fusion. The repulsive force between positively charged nuclei, known as the Coulomb barrier, must be overcome for fusion to occur, and this requires incredibly high energy (400 keV for two protons, for example) [1-2]. The process of nuclear fusion takes 100 million degrees. Due to its infinite fuel supply, nuclear fusion is therefore the preferable method for current and upcoming research. For example, transient radioactive waste is produced during the operations of safe fusion reactors [3-6]. Tritium and deuterium are used in the most well-known fusion reaction. Turbine steam is created when water is warmed by the 14 MeV neutron from this event. Moreover, 3.5 MeV He is produced by this reaction. Under extreme heat, the fusion product reactor's generated helium serves as the input nuclei for deuterium and tritium [7-11]. Plasma, a conductive ionized gas, is controlled by magnetic confinement in fusion reactors. However, a significant problem is plasma-wall interaction, which weakens reactor walls through heat, particle impact, and gas absorption, lowering lifespan and efficiency (Figure 1).

Figure 1: WEST, the tokamak of the CEA [12]

Tritium retention in materials that face plasma, like graphene, is another crucial problem; studies in reactors like JET and TFTR have shown retention rates of 40–51%. ITER may approach its tritium limit in roughly 100 pulses, according to simulations, which would degrade walls and reduce efficiency. Tritium bombardment on graphene showed increased wall breakdown in molecular dynamics simulations, underscoring the need for better materials. Future studies will concentrate on improving reactor designs and materials that face plasma in order to increase their longevity and effectiveness for energy and space applications. While plasma-wall damage, tritium retention, and material deterioration are difficulties, clean, almost unlimited fuel is a key feature that makes it perfect for high-power space missions [12]. Optimized reactor designs and improved materials like graphene are needed for solutions, and future research will focus on simulations and tests to forecast and lessen degradation. According to new research on the retention of tritium in graphene-based tokamak wall designs, graphene coatings may offer several advantages over more traditional materials like tungsten or carbon composites. Compared to graphite, few-layer graphene can reduce tritium retention by as much as 70% due to its high diffusion rates and poor hydrogen isotope solubility, which encourage tritium desorption [13-22]. Tritium ion plasma penetration on the graphene crystal surfaces was modeled using molecular dynamics simulations in order to investigate this. The interactions are subjected to stochastic analysis from a chemical standpoint. The findings indicated that tritium retention shortens reactor lifetime by speeding up wall deterioration.

Method

The Python programming language was used to perform molecular dynamics simulations. This work was accomplished using Spyder, a component of the Anaconda module, version 6.0.3. Calculations were carried out using a Dell Precision 7680 running Ubuntu 24.10 Linux and outfitted with an Intel Core i7 13th Generation processor. The Python compiler version used was 3.12.7. In this work, a Python framework for molecular dynamics simulations called the Atomic Simulation Environment (ASE [23]) is used (Figure 2).

Figure 2: Atomic Simulation Environment in Python language for Molecular Dynamics Simulation

In the molecular dynamics simulation, a sizable portion of graphene—roughly 1,200 carbon atoms—is simulated in order to develop the kinetic energy-based Shannon Entropy. An analysis of the tritium ion plasma penetration's chemical consequences on the graphene crystal is conducted. This analysis evaluates bonding, process conditions, and atom boundary conditions. The results hold significant ramifications for forthcoming investigations into carbon-based materials and their multifarious uses in numerous industries. It is assumed that graphene has a C hexagonal crystal structure. Tritium is addressed with single hydrogen atoms for the sake of simplicity in the scale of the simulated material molecular calculations. The tritium (hydrogen) atoms in (Figure 3) are shown as white in the molecular dynamics, whereas the carbon atoms are represented as gray. To facilitate computations and replace tritium, the block was exposed to hydrogen at energy levels ranging from 5 to 35 keV using 3T magnetic induction. According to the literature, the current simulations encompass an appropriate range of collision energy, proving that the energy levels chosen for the simulation were sufficient.

How to cite this article: Alper Pahsa. Chemical Analysis of a Tritium Plasma Graphene Interactions with Stochastic Approaches. Eng Technol Open Acc 2025; 6(4): 555693. DOI: 10.19080/ETOAJ.2025.06.555693

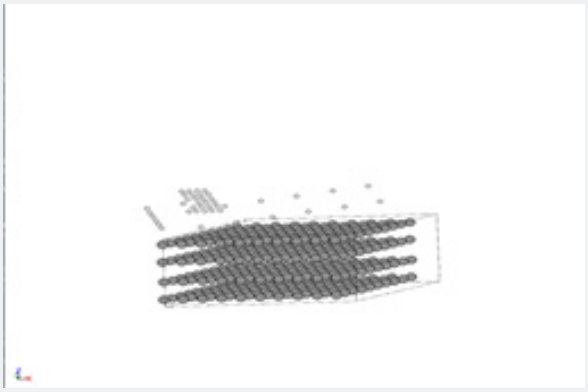

Figure 3: 3D representation of tritium ions on the graphene surface

The initialization of the molecular dynamics are given as below:

- a1 = 2.46 #Lattice constant for graphen (in Angstrom)
- c1 = 6.70 #Interlayer spacing for graphen (in Angstrom)
- num_hydrogen_atoms = 42
- timestep = 1.0 # femto second
- total_steps = 200
- temperature = 300 K
- bulk_cutoff = 5.0 (Distance cutoff for retention (Angstroms))
- hydrogen_mass = 1.00784* 1.66053906660e-27* units.kg (Mass of hydrogen atom)

The Effective Medium Theory (EMT) potential specified in the ASE Python framework serves as interatomic potential for the simulation configurations of the materials used in this investigation. Averaging the various values of the constituents that directly comprise the composite materials in an electromagnetic environment is how EMT is created given in the literature. The overall materials' effective permittivity is computed using reasonable approximations. Under controlled circumstances, thermal equilibrations were carried out at 300K using leftover graphene. These were carried out in considerable numbers. The microcanonical (NVE) ensemble's magnetic force impacts allowed the surface layers to move freely for a single second. This facilitated the movement of these layers. The mechanism that maintains the energy, volume, and elements of the ensemble at consistent levels makes this possible. The heat produced by the bombardment was dispersed by Langevin-thermostatizing the top four layers for one picosecond following the NVE cycle.

A thermally regulated graphite block in a vacuum (~3 Å) was used to study the effects of hydrogen (5–35 keV) on graphene using molecular dynamics simulations. Atoms were able to escape, but movement was restricted by periodic limits. The force field is a set of energy functions that help us understand the energy involved in the interaction between atoms; it is usually the sum of covalent and non-covalent interactions among the atoms and molecules, or bonded and non-bonded terms. It is necessary to first develop a precise understanding of the force field in order to compute the forces acting on the atoms, which are the functional form of potential energy.

The formulation of the force field is:

$$U(r) = U_{bonded} + U_{non-bonded} \quad (1)$$

Bonded Interactions (Covelent terms): This item explains how atoms made of chemical bonds interact with one another.

- Bond stretching (Harmonic oscillator approximation):

$$U_{bond} = \sum_{bonds} \frac{1}{2} k_b (r - r_o)^2 \quad (2)$$

in (2); =bond force constant, r=instantaneous bond length, =equilibrium bond length

- Torsional rotation (Dihedral potential)

$$U_{dihedral} = \sum_{dihedral} k_\Phi (1 + cos(n\Phi - \delta))^2 \quad (3)$$

in (3); =dihedral force constant, n=periodicity (multiplicity), =dihedral angle, =phase shift

- Angle bending (Harmonic potential)

$$U_{angle} = \sum_{angles} \frac{1}{2} k_\theta (\theta - \theta_0)^2 \quad (4)$$

in (4); k_θ=angle force constant, θ=instantenous bond angle, θ_0=equilibrium angle.

- Improper dihedrals (Out-of-plane bending)

$$U_{improper} = \sum_{impropers} \frac{1}{2} k_\psi (\psi + \psi_0)^2 \quad (5)$$

in (5); is the improper angle (i.e. maintaining planarity in aromatic rings)

Non-Bonded Interactions (Non-Covelent Terms): These explain how atoms that are not directly bound interact:

- van der Waals (Lennard-Jones potential)

How to cite this article: Alper Pahsa. Chemical Analysis of a Tritium Plasma Graphene Interactions with Stochastic Approaches. Eng Technol Open Acc 2025; 6(4): 555693. DOI: 10.19080/ETOAJ.2025.06.555693

$$U_{vdW} = \sum_{i<j} 4\epsilon_{ij}\left[\left(\frac{\sigma_{ij}}{r_{ij}}\right)^{12} - \left(\frac{\sigma_{ij}}{r_{ij}}\right)^{6}\right] \quad (6)$$

in (6); =depth of the potential well, =distance at which U=0, =distance between atoms i and j

- Electrostatic (Coulomb potential)

$$U_{elec} = \sum_{i<j} \frac{q_i q_j}{4\pi\epsilon_0 r_{ij}} \quad (7)$$

in (7); , =partial atomic charges, =vacuum permittivity, =distance between charges

Complete Force Field Equation: When all terms are added together, a typical force field (such as AMBER, CHARMM, or OPLS) is represented as follows:

$$U(r) = \sum_{bonds}\frac{1}{2}k_b(r-r_0)^2 + \sum_{angles}\frac{1}{2}k_\theta(\theta_0-\theta_0)^2 + \sum_{dihedrals}\frac{1}{2}k_\phi(1+\cos(n\Phi-\delta)) + \sum_{dihedral}k_\phi(1+\cos(n\Phi-\delta))^{\square} + \sum_{impropers}\frac{1}{2}k_\psi(\psi+\psi_0)^2 + \sum_{i<j}4\epsilon_{ij}\left[\left(\frac{\sigma_{ij}}{r_{ij}}\right)^{12} - \left(\frac{\sigma_{ij}}{r_{ij}}\right)^{6}\right] + \sum_{i<j}\frac{q_i q_j}{4\pi\epsilon_0 r_{ij}} \quad (8)$$

The force constants (kb, kθ, kϕ, kψ) and parameters (ϵ,σ, q) are empirically or quantum mechanically computed for particular force fields, whereas the non-bonded terms in (8) have the power of intermolecular forces and long-range interactions. The bonded terms in (8) preserve molecular structure. This approach enables the Molecular Dynamic simulations to use Newton's equations to propagate atomic motions and calculate forces in (9).

$$m_i r_i = -\frac{\delta u}{\delta r_i} \quad (9)$$

To do this in (9) computation, the forces acting on the atoms which are usually derived from a potential energy—need to be known numerically for the entire geometrical set of 3N atomic coordinates . The basic graphene layer remained at 300K after absorbing motion. The top four layers evolved freely for a brief period of time (NVE ensemble, 1 fs) prior to heat dissipation (1 ps thermostating), while layers 2–8 were thermostated at 300K during bombardment. Faster thermostating was necessary because van der Waals interactions were too slow. While capturing collision dynamics, femtosecond timesteps guaranteed computational viability. This simulation uses the potential energy of the simulation box to calculate the Shannon Entropy of the system's atom locations and the Shannon Entropy of the potential energy of the retention of tritium plasma ions. Shannon states that p1, p2, p3,..., pn are the set of probabilities that produce vagueness via (H) measurement. When the atom locations and system potential energy indicated in this system model are put into practice, the Shannon Entropy is as follows [24]:

$$H = K\sum_{i=1}^{n} p_i log_2 p_i \quad (10)$$

The transformation coefficient is K, and the Shannon Entropy contains the following probabilities: p1, p2, p3,..., pn. In molecular dynamics, equation (2) above provides the frequency of the simulation box's potential energy as well as the atom locations that are seen inside the system configuration atom model. When thermal equilibration was complete, post-impact analysis proceeded.

Results and Discussion

Through the use of a 3T magnetic induction, the simulation bombards the graphene crystal with hydrogen ions at energies between 5 and 35 keV. The next step of the process is to run simulations of molecular dynamics. Thermostat integration is made easier by the several layers of graphene fabrication. This sequence illustrates the Shannon Entropy based on the results of three-dimensional molecular dynamics simulations and the molecular configuration's kinetic energy estimates. (Tables 1-4) display the simulation length as well as the Shannon Entropy for tritium based on kinetic energy using a 3T electromagnetic force and kinetic energies ranging from 5 keV to 35 keV. (Figures 4 -7) shows the Shannon Energy based Kinetic Energy versus simulation time graphs for the energies ranging from 5 keV to 35 keV. Since the simulations involve kinetic energy (KE) distributions of tritium ions impacting graphene, it can be related to the Shannon Entropy (H) of Kinetic Energy to system disorder and energy-dependent reaction probabilities. The Shannon Entropy (10) was computed for different KE bombardments (5-35 keV). The observed key parameters are: (Table 5)

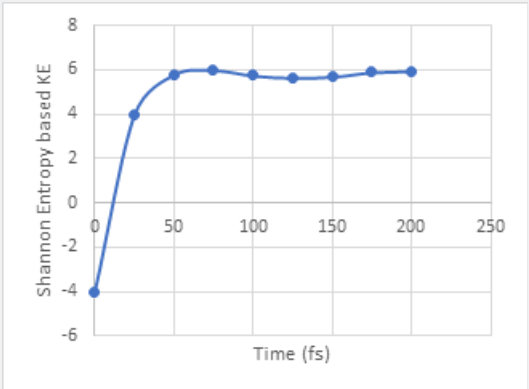

Figure 4: Shannon Entropy based on KE vs Time for 5 keV tritium plasma penetration

How to cite this article: Alper Pahsa. Chemical Analysis of a Tritium Plasma Graphene Interactions with Stochastic Approaches. Eng Technol Open Acc 2025; 6(4): 555693. DOI: 10.19080/ETOAJ.2025.06.555693

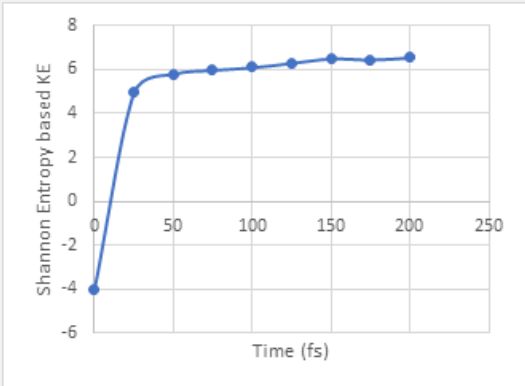

Figure 5: Shannon Entropy based on KE vs Time for 15 keV tritium plasma penetration

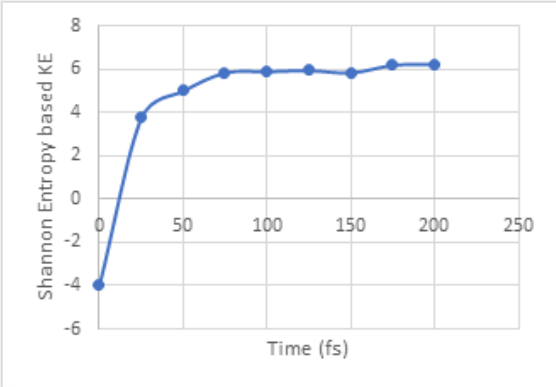

Figure 6: Shannon Entropy based on KE vs Time for 25 keV tritium plasma penetration

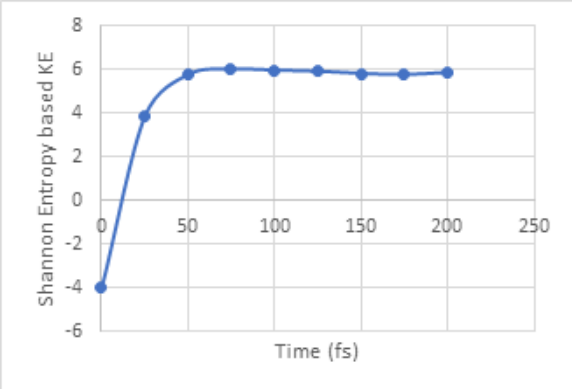

Figure 7: Shannon Entropy based on KE vs Time for 35 keV tritium plasma penetration

How to cite this article: Alper Pahsa. Chemical Analysis of a Tritium Plasma Graphene Interactions with Stochastic Approaches. Eng Technol Open Acc 2025; 6(4): 555693. DOI: 10.19080/ETOAJ.2025.06.555693

Table 1: Kinetic energy-based Shannon Entropy values calculated by equation 10 for Tritium with 5keV bombardment with 3T on Graphene Crystal.

Process Time (fs)	Kinetic Energy Shannon Entropy of the total bulk surface
0	-4
25	4
50	5,8
75	6
100	5,75
125	5,65
150	5,7
175	5,9
200	5,95

Table 2: Kinetic energy-based Shannon Entropy values calculated by equation 10 for Tritium with 15keV bombardment with 3T on Graphene Crystal

Process Time (fs)	Kinetic Energy Shannon Entropy of the total bulk surface
0	-4
25	4,95
50	5,8
75	5,98
100	6,1
125	6,3
150	6,5
175	6,45
200	6,55

Table 3: Kinetic energy-based Shannon Entropy values calculated by equations 10 for Tritium with 25keV bombardment with 3T on Graphene Crystal

Process Time (fs)	Kinetic Energy Shannon Entropy of the total bulk surface
0	-4
25	3,75
50	5
75	5,85
100	5,9
125	5,95
150	5,85
175	6,2
200	6,25

Table 4: Kinetic energy-based Shannon Entropy values calculated by equations 10 bombardment with 3T on Graphene Crystal.

Process Time (fs)	Kinetic Energy Shannon Entropy of the total bulk surface
0	-4
25	3,85
50	5,75
75	6
100	5,95
125	5,9
150	5,8
175	5,75
200	5,85

How to cite this article: Alper Pahsa. Chemical Analysis of a Tritium Plasma Graphene Interactions with Stochastic Approaches. Eng Technol Open Acc 2025; 6(4): 555693. DOI: 10.19080/ETOAJ.2025.06.555693

Table 5: Observations of the key parameters for the Shannon Entropy based on Kinetic Energy

KE (keV)	Initial H (0 fs)	Peak H (fs)	Final H (200 fs)	Trend
5	-4	6.00 (75 fs)	5.95	Rapid rise, then stabilization
15	-4	6.55 (200 fs)	6.55	Steady increase
25	-4	6.25 (200 fs)	6.25	Gradual rise
35	-4	6.00 (75 fs)	5.85	Rise, then slight decline

According to the main conclusions, the system first displays a highly ordered state, as shown by the negative entropy (H = -4 at 0 fs), which is uncommon but feasible in systems with constraints like pure graphene. Entropy evolution changes with ion energy over time: a 5 keV bombardment causes stabilization (~5.95) after a quick entropy increase (H = 6 at 75 fs), whereas a 15 keV bombardment causes continual disorder (H = 6.55 at 200 fs) because of deeper ion penetration. There are entropy peaks at higher energies (25-35 keV) with small reductions, which could be caused by lattice recovery or ion reflection. Greater entropy and reaction probability (k) are correlated with higher kinetic energy (15-35 keV) as compared to Arrhenius behavior; however, nonlinear patterns imply saturation effects such as defect saturation. According to transition state theory, the maximum reaction probability is represented by the peak entropy (H), and greater disorder implies a lower effective activation energy (E_a). In particular, the lowest E_a for defect production is suggested by a 15 keV bombardment (H = 6.55). Force field approximations, finite timesteps, and periodic boundary conditions all introduce uncertainty, therefore additional validation using duplicated simulations with various random seeds and DFT comparisons is required for more precise E_a calculation.

Conclusion

The tritium (H) retention activity that would take place inside the graphene crystal structure in fusion reactor walls was better understood as a conceptual research through the use of Shannon Entropy of atom locations and Shannon Entropy calculated using the kinetic energy data previously mentioned. Molecular dynamics has helped us better grasp the forces, fusion conditions, and energy that result in the atomic activities of material formations. Due to the potential and kinetic energies of the various graphene crystal structure layers in the established molecular dynamics, the retention of the tritium plasma ion increases as its kinetic energy (5,15,25, and 35 keV) increases on the graphene wall's surface. Shannon Entropy analysis of tritium-graphene interactions reveals an energy-dependent increase in disorder, with 15 keV bombardment inducing the highest entropy, indicating optimal conditions for defect formation. An Arrhenius-type analysis further suggests a lower effective activation energy (EaEa) at higher kinetic energies, though saturation effects become apparent beyond 25 keV. Future work will focus on extending simulations to elevated temperatures (500-1000 K) to construct more comprehensive Arrhenius plots, while incorporating quantum corrections for improved Ea predictions. Additionally, experimental validation through plasma-graphene interaction studies will be pursued to verify computational findings and refine the theoretical framework.

Acknowledgment

This study is being supported by Havelsan Inc.'s research and development division.

Declarations

During the investigation, no conflicts of interest, either financial or non-financial, were discovered. The study did not meet the ethical standards established by recognized publication and research protocols since neither human nor animal subjects provided their informed consent.

Data Availability

The findings of the investigation are backed up by the text and other materials. The related author may supply more information pertinent to the inquiry upon reasonable request.

References

1. Ongena J (2016) Nuclear fusion and its large potential for the future world energy supply. Nukleonika Journal 61(4): 425-432.
2. Takeda S, Pearson R (2018) Nuclear Fusion Power Plants.Power Plants in the Industry. IntechOpen publishing.
3. IAEA (2018) Fusion Energy for Peace and Sustainable Development. IAEA. Vienna 2-18.
4. Kikuchi M, Lackner K, Tran MQ (2012) Fusion Physics. IAEA. Vienna 20-21
5. Ibrahim S, Lahboub FZ, Brault P, Petit A, Caillard A et al., (2021) Influence of helium incorporation on growth process and properties of aluminum thin films deposited by DC Magnetron sputtering. Surface and Coatings Technology 426.
6. Behrish R, Harries DR (1986) International Atomic Energy Agency. Lifetime Predictions for The First Wall and Blanket Structure of Fusion Reactors. Nuclear Fusion J 26(5).
7. Nuclear Fusion (2002) Half a Century of Magnetic Confinement Fusion Research. IoP Publishing Ltd. 230-258.
8. Jones ES, Rafelski J (1987) Cold Nuclear Fusion. Scientific American. Springer Nature Publishing. 66-71.
9. Kajita S, Kawaguchi, Ohno N, Yoshida N (2018) Enhanced growth of large-scale nanostructures with mettalic ion precipitation in helium plasmas. Scientific Reports.

How to cite this article: Alper Pahsa. Chemical Analysis of a Tritium Plasma Graphene Interactions with Stochastic Approaches. Eng Technol Open Acc 2025; 6(4): 555693. DOI: 10.19080/ETOAJ.2025.06.555693

10. Kotov V (2017) Particle conservation in numerical models of the tokamak plasma edge. Physics Plasma 24(4).

11. K Wojcyzkowski (2011) New Development in Corrosion Testing: Theory, Methods and Standards. AESF Foundation, Plating and Surface Finishing.

12. Andrei M, (2025) France Fusion Reactor Breaks Record for Plasma Duration, ZME SCIENCE.

13. L Rajablou, SM Motevalli, F Fadaei (2022) Study of alpha particle concentration effects as the ash of deuterium-tritium fusion reaction on ignition criteria. Physica Scripta 97(9).

14. Malo M, Morono A, Hodgson ER (2016) Plasma Etching to Enhance the Surface Insulating Stability of Aluminumina for Fusion Applications. Nuclear Materials and Energy. Elsevier 9: 247-250.

15. McFadden C, (2023) Tokamak Energy has just made a breakthrough in nuclear fusion. Interesting Engineering.

16. Nadler J (1995) Inertial-Electrostatic Confinement (IEC) of A Fusion Plasma with Grids. Nuclear Engineering Department. University of Illinois.

17. Nordlund K (2006) Atomistic Simulations of Plasma-wall interactions in Fusion Reactors. Physica Scripta. T124: 53-57.

18. Ongena J (2016) Nuclear fusion and its large potential for the future world energy supply. Nukleonika Journal 61(4): 425-432.

19. Perrault D (2017) Nuclear Fusion Reactors-Safety and Radiation Protection Considerations for Demonstration Reactors that follow ITER facility. IRSN.

20. Arena P, Maio (2020) PA Special Issue.Structural and Thermo-Mechanical Analysis in Nuclear Fusion Reactors. MDPI Applied Sciences 12(24).

21. Freidberg JP, Mangiarotti FJ, Minervini (2015) Designing a Tokamak Fusion Reactor-How Does Plasma Physics Fit In? AIP Publishing 22(7).

22. Fusion Energy Sciences Workshop on Plasma Material Interactions-Report on Science Challenges and Research Opportunities in Plasma Material Interactions. (2015) Office of Science, Fusion Energy Sciences.

23. Ask Hjorth Larsen, Jens Jørgen Mortensen, Jakob Blomqvist, Ivano E Castelli, Rune Christensen, et al. (2017) The Atomic Simulation Environment-A Python library for working with atoms. Phys.: Condense Matter 29(27): 273002.

24. Karaca Y, Moonis M (2022) Multi-Chaos, Fractal and Multi-Fractional Artificial Intelligence of Different Complex Systems. Academic Press 231-245.

DOI: 10.19080/ETOAJ.2025.06.555693

How to cite this article: Alper Pahsa. Chemical Analysis of a Tritium Plasma Graphene Interactions with Stochastic Approaches. Eng Technol Open Acc 2025; 6(4): 555693. DOI: 10.19080/ETOAJ.2025.06.555693